Journal of Alloys and Compounds 509 (2011) 4171–4175

Contents lists available at ScienceDirect

Journal of Alloys and Compounds

journal homepage: www.elsevier.com/locate/jallcom

Electronic structure and thermal properties of doped $CaMnO_3$ systems

F.P. Zhang*, X. Zhang, Q.M. Lu, J.X. Zhang, Y.Q. Liu

Key Laboratory of Advanced Functional Materials, Chinese Ministry of Education, College of Materials Science and Engineering, Beijing University of Technology, 100124, Beijing, People's Republic of China

ARTICLE INFO

Article history:
Received 9 November 2010
Received in revised form 4 January 2011
Accepted 4 January 2011
Available online 12 January 2011

Keywords:
$CaMnO_3$
First principle calculation
Electronic properties
Thermal properties

ABSTRACT

The electronic and thermal properties of hole (Na) and electron (Ga) doped $CaMnO_3$ systems are investigated based on the first principle density functional theory calculations using plane wave basis and pseudo-potential method. A semiconductor-to-conductor transition and a distorted band structure are found for the doped systems; enhanced density of states near Fermi level is observed. The phonon transfer speed and the phonon mean free path are lowered; meanwhile, the phonon specific heat is heightened in comparison with that of the undoped $CaMnO_3$ system, resulting in enhanced phonon thermal conduction. The calculation results indicate that the doped systems should have improved thermoelectric performance.

1. Introduction

The $AMnO_3$ oxides (A = Ca, La, Sr, Ba) with perovskite type structure have attracted much attention due to their variety of physical properties [1–4]. The $AMnO_3$ structure can be described with corner sharing octahedra, in which Mn is surrounded by six oxygens and A locates in cavities. Dopants can be incorporated into the $AMnO_3$ structure [5,6], leading to extensive variation of chemical and physical properties. Understanding the doping behavior is significative for the optimization of electronic materials [4,7,8].

As one of these type oxides, the $CaMnO_3$ based manganite has renewed interest within solid state fields in terms of their structural [7,8], electrical [9], magnetic [10] and thermoelectric (TE) properties [11,12]. The physical behavior of carrier doped $CaMnO_3$ has been widely studied in an attempt to understand the rich variations of physical properties. It is true that the physical properties can be sensitively influenced by donor doping, the dopants include main group elements, transitional metal elements and rare earth elements [13–16]. The $CaMnO_3$ manganite shows n-type semiconductor transportation up to room temperature, electron donor doping is thought to be applicable for increasing the carrier concentration, tuning the mobility, effective mass and mean free path and the conduction behavior thereby. Meanwhile, structural distortion could be induced by dopants; the electronic structure as well as the phonon mode could be changed consequently. There were a large number of experimental investigations on doped $CaMnO_3$ with trivalent or tetravalent ions substitution (La, Ce, Nd, Sm and Yb) for Ca site [11,17]. The carrier concentration modification, structural variation, orbital coupling change and ion electronic configuration modulation was thought to be responsible for the physical property fluctuations. It was reported [18] that the carrier concentration can be adjusted by electron donor dopants; the inter-site distance for carriers to conduct can be modified and the carrier conduction capability can thus be tuned by dopants. Funahashi and co-workers [17,19] investigated the Seebeck signals of doped $CaMnO_3$ systems, they believed that the Mn 3*d* electron orbital and the symmetry of Mn–O–Mn octahedron were affected by donor dopants. Those meaningful physical variations are deeply complicated; they deserve further detailed investigation.

The electrical properties of solid state materials are determined by their electronic structures; however, there were few reports on the detailed electronic structure study of doped $CaMnO_3$ systems. Zampieri et al. [20] investigated the electronic structure of hole doped $CaMnO_3$ systems and they found that the ground state of the manganite was highly covalent, the main separation between Mn 3*d* bands closest to Fermi level was of the order of 3 eV. Briático [21] measured conductivity and magnetic properties of electron doped $CaMnO_3$ system and they found that the Curie constant was dependent on doped electron concentration; they believed that the formed Mn^{3+}–Mn^{4+} spin clusters were responsible for the large Curie constant. A few theoretical works in terms of $CaMnO_3$ system had been reported. Yang et al. [22] studied electronic structure of anti-feromagnetic $CaMnO_3$ using the first principle discrete variational cluster method based on ab initio local-spin-density approximations, a band gap of 0.005–0.1 eV for the titled system was found. Recently, we carried out density functional theory study on anti-ferromagnetic $CaMnO_3$ and an indirect band gap of 0.7 eV was revealed [23]. Nevertheless, detailed investigations are needed

* Corresponding author. Tel.: +86 10 67392661; fax: +86 10 67392840.
E-mail addresses: zhfp@emails.bjut.edu.cn, zhfpeng@yahoo.com.cn (F.P. Zhang).

0925-8388/$ – see front matter © 2011 Elsevier B.V. All rights reserved.
doi:10.1016/j.jallcom.2011.01.032

Table 1
Lattice parameters of undoped, Na and Ga doped $CaMnO_3$.

Parameters	Na doped $CaMnO_3$	$CaMnO_3$	Ga doped $CaMnO_3$
a	10.1594	10.6386	10.6116
b	7.3265	7.4148	7.1845
c	5.0782	5.2093	5.3922
Bond lengths			
Mn–O1	1.802	1.926	2.083
	1.799	1.918	1.687
Mn–O2	1.828	1.916	1.798

to understand the doping properties of $CaMnO_3$ system. In this paper, we report the systematical density functional theory (DFT) calculation results for both hole and electron doped $CaMnO_3$ systems; the electrical properties as well as the thermal properties are analyzed. In the end, the TE properties are prospected.

2. Computational details

The crystal structure of $CaMnO_3$ in our calculations can be found in Refs. [23,24]. Na as hole and Ga as electron donor dopants were chosen to investigate the electronic state evolution. Super cells with a size of 40-atom corresponding to the formula $Ca_{0.875}M_{0.125}MnO_3$ (M = Na, Ga) were considered in this study. Calculations on large supercell were beyond computing capability.

Our calculations were performed with the ultra-soft pseudopotential plane wave method and generalized gradient approximations (GGA) based on DFT theory using the Cambridge Serial Total Energy Package (CASTEP, Cerius2, Molecular Simulation, Inc.) ab Initio Total Energy Program [25,26]. Energy cutoffs of 340 eV and 220 eV were used for the geometric optimization, band structure and phonon calculations, respectively. The wave functions sample the irreducible part of the Brillion zone with sets including 15 points (Monkhorst-Pack grid $2 \times 3 \times 5$), the band energy tolerance was set as 0.01 meV. The electronic structure was analyzed in terms of the band structure, density of states and charge distribution. The high symmetry *k*-points within our calculated band structure in the Brillouin zone were *G*(0.000, 0.000, 0.000), *F*(0.000, 0.500, 0.000), *Q*(0.000, 0.500, 0.500), *Z*(0.000, 0.000, 0.500). The thermodynamic parameters, Debye temperature Θ and thermal capacity *c* as a function of temperature were obtained from phonon dispersion calculations. The phonon density of states was obtained from phonon calculations. Then the thermal property was analyzed in terms of the phonon calculation results.

3. Results and discussion

3.1. Geometric structure

Table 1 shows the geometrically optimized structure parameters of the undoped $CaMnO_3$ and doped $CaMnO_3$ systems. The lattice parameters *a*, *b* and *c* are changed due to the introducing of dopants with different ionic radii. The main conduction path Mn–O length turns out to be changed too, indicating the modified electronic properties; i.e. the Mn–O1 length is reduced to be 1.802 Å and 1.799 Å of Na doped $CaMnO_3$ system from 1.926 Å and 1.918 Å of undoped $CaMnO_3$ system, respectively.

3.2. Electronic properties

Fig. 1 shows the band structures of the undoped $CaMnO_3$ and doped $CaMnO_3$ systems. The Fermi level is set to be 0 eV and other energy levels are determined by comparing with Fermi level. The Fermi levels of the doped systems shift upwards into the conduction bands due to the carriers arising from doping, indicating a

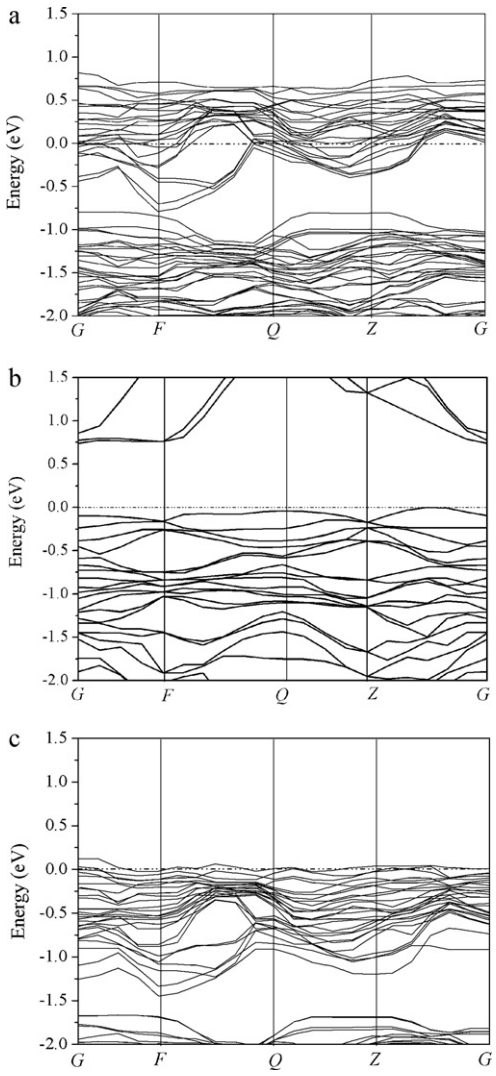

Fig. 1. Calculated energy band structures of undoped (b), Na (a) and Ga (c) doped $CaMnO_3$.

semiconductor-to-conductor transition. Thus the doped systems become metallic. Fig. 2 shows the total density of states (TDOS) and partial density of states for species within each system. It is inferred that the energy for carriers to hop would be reduced in the doped systems.

As can be seen for doped $CaMnO_3$ systems, our calculation also indicates that the Mn*d* and O*p* orbitals mainly contribute to the energy states near Fermi level (see Fig. 2) [23]. The Mn*d* and O*p* electrons and their couplings are responsible for electronic process for doped $CaMnO_3$ systems [13–19]. Moreover, an enhanced hybridization between the Mn*d* and O*p* electrons is observed for the doped systems, enhanced electron conduction can be expected, since the Mn–O path is the main conduction path.

3.3. Thermal properties

The Debye temperature Θ and specific heat *c* characterize the thermodynamic property of the crystalloid phase materials. The Debye temperature Θ is associated with phonon transfer speed *v* as:

$$\Theta = \frac{\hbar v}{k_B}(6\pi^2 N)^{1/3} \quad (1)$$

where *N* is the number of atoms per unit cell [27]. Fig. 3 presents the calculated Debye temperature Θ of all systems, the calculation

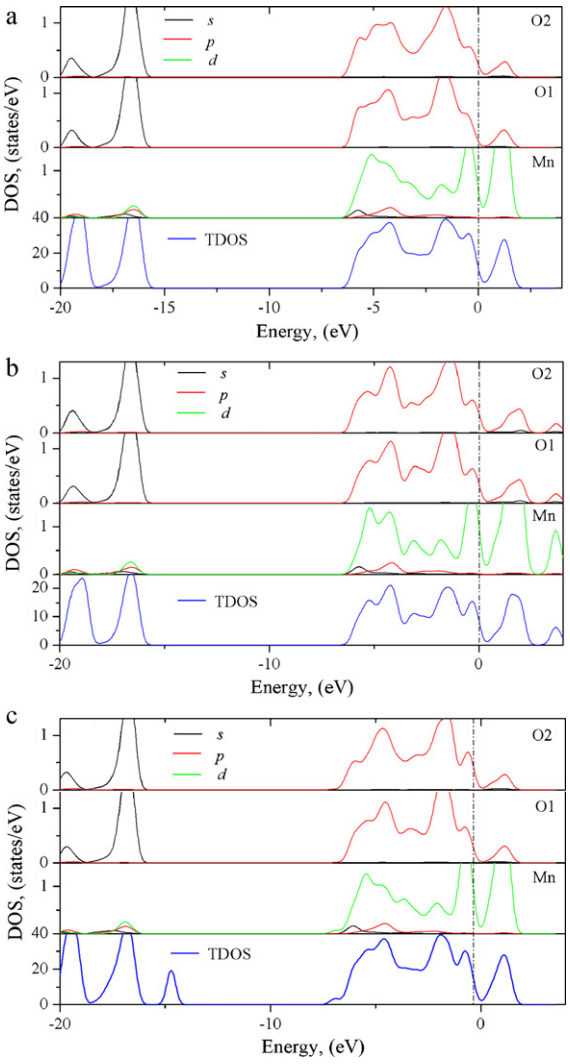

Fig. 2. Density of states of undoped (b), Na (a) and Ga (c) doped $CaMnO_3$.

detail could be found elsewhere [28]. Within very low temperature region (<50 K), the Debye temperature of the undoped system is lower than that of the doped systems; then the Debye temperature Θ of doped systems gets lower than that of the undoped system. Since the phonon transfer speed v correlates positively with Debye temperature Θ, the phonon transfer speed v for doped systems is inferred to be heightened at low temperature and is lowered at high temperature.

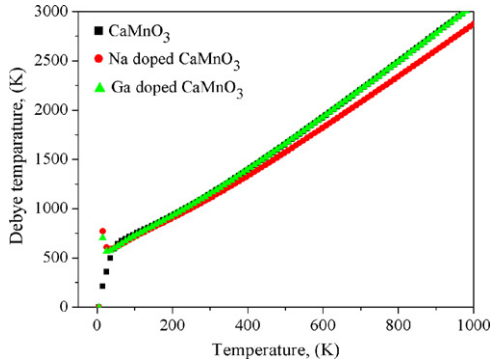

Fig. 3. Calculated Debye temperature Θ of all systems.

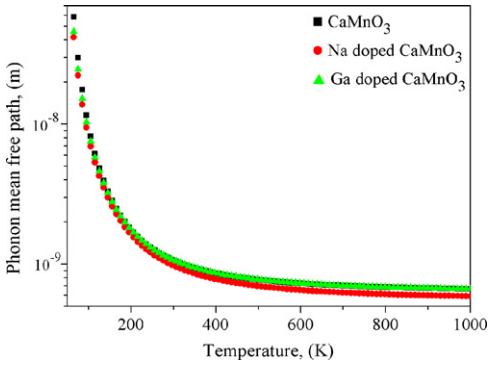

Fig. 4. Calculated phonon mean free path l_p of all systems.

The phonon mean free path l_p can be figured out by associating with Debye temperature:

$$l_p = 10^8 \exp\left(\frac{\Theta}{\eta T}\right) \quad (2)$$

where η is a constant and T is absolute temperature [29]. Fig. 4 presents the calculated mean free path l_p of all systems. It is observed that the phonon mean free path l_p is lowered.

Within the low-order approximation, the phonon thermal conductivity k_p could be expressed as a function of specific heat c, phonon transfer speed v and phonon mean free path l_p [27]:

$$k_p = \frac{1}{3} c v l_p \quad (3)$$

The k_p could be obtained based on the calculated c, v and l_p values. Fig. 5 presents the calculated lattice specific heat c and phonon thermal conductivities k_p of all systems. It could be seen that both the lattice specific heat c and the phonon thermal conductivity k_p are increased. The temperature dependence of k_p is in good agree-

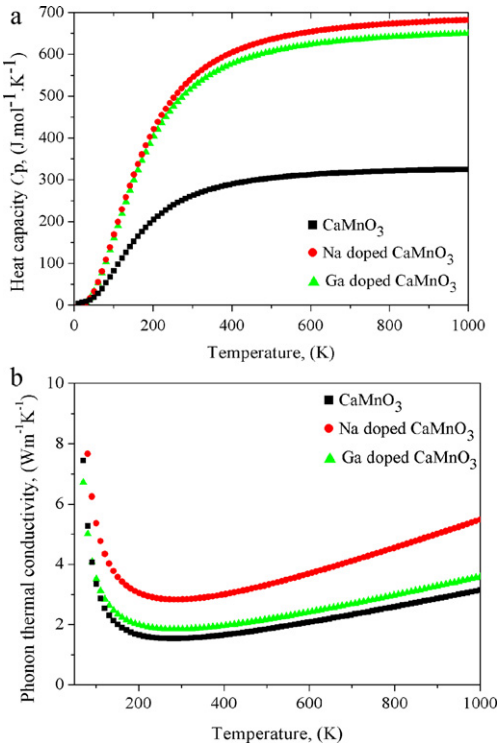

Fig. 5. Calculated lattice specific heat c (a) and phonon thermal conductivity (b) of all systems.

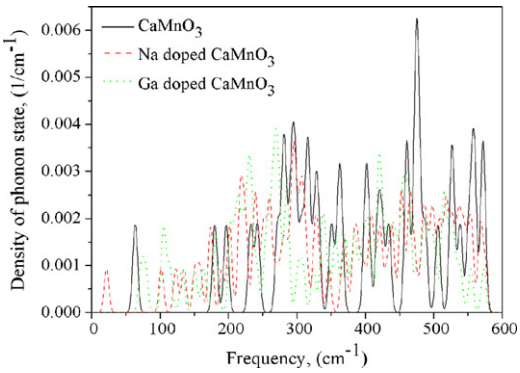

Fig. 6. Calculated phonon density of states of all systems.

ment with experimental results of $CaMnO_3$-based materials [30]. Secondly, the phonon thermal conductivity of Na doped $CaMnO_3$ oxide is increased, which is also in good agreement with experimental results of Na doped oxides [31]. These results verify the applicability of the calculation models. Furthermore, the phonon thermal conductivity of Na doped system is higher than that of the Ga doped system. To further understand the phonon states, Fig. 6 shows the calculated phonon density of states of all systems. It could be easily seen that the states of the frequency for the doped system are densely distributed in the whole frequency region, and the density of phonon states of Na doped system is higher than that of the Ga doped system. The dopant Na(Ga) coordinates with twelve anions within the system, the much more intensive combination and shorter bond length [29] of Na doped system is estimated to be responsible for its higher phonon specific heat and the phonon thermal conductivity.

3.4. Prospects of TE properties

The performance of a TE material is determined by the dimensionless figure of merit ZT:

$$ZT = \frac{\alpha^2 T}{\rho k} \tag{4}$$

In which the α, ρ, T and k characterizes the Seebeck coefficient, carrier conduction capability, absolute temperature and thermal conduction capability, respectively [1]. The $CaMnO_3$-based systems are potential n-type TE materials [11,12]. Here we discuss the TE properties of the two light elements doped systems. According to Boltzman transport theory [32], the absolute Seebeck coefficient α of $CaMnO_3$ system could be deduced as:

$$\alpha \propto c\frac{k_B^2}{e}\left(\frac{1}{n}\right)^{2/3} Tm^* \tag{5}$$

where α is Seebeck coefficient, k_B is Boltzmann constant, e is elementary charge, n is carrier density, m^* is carrier effective mass, c is an integrated constant and T is absolute temperature [33,34]. At certain temperatures, the Seebeck coefficient should be a function of carrier density n and carrier effective mass m^*. As shown in the band structures, the bands near Fermi level are distorted. It could be observed that the effective mass m^* is enhanced. It can be deduced that the Seebeck coefficient of Na doped system should be enhanced; while the Seebeck coefficient of the Ga doped system would be a compromise of carrier density n and effective mass m^*. Within the low doping concentration, the carrier density n would not be changed intensively ($Ga^{1.39+}$). The Seebeck coefficient of Ga doped system should be hopefully maintained. In addition, the combinations of heavy and light carriers for doped $CaMnO_3$ systems should also contribute to TE properties [35]. Although experiment should be done to evaluate the TE properties of the doped systems, the Ga doped $CaMnO_3$ system is expected to have improved TE performance due to enhanced carrier conduction capability, hopefully maintained Seebeck coefficient and slightly increased phonon thermal conductivity.

4. Conclusions

In the present work, we have performed the first principle calculations for light elements doped $CaMnO_3$ perovkite systems in terms of their electronic structures and thermal properties. Both the hole and electron doped systems undergo a semiconductor-to-conductor transition and a band structure distortion. The density of states near Fermi level is increased, the carrier conduction capability is observed to be enhanced; the phonon mean free path and the phonon transfer speed are decreased, while the phonon specific heat and the phonon thermal conductivity are increased for both doped systems. Improved thermoelectric performances are indicated for the doped systems.

Acknowledgements

The present work is financially supported by the National Natural Science Foundation of China under Grant Nos. 50702003 and 50801002, the Beijing Municipal Commission of Education Foundation under Grant No. JC009001200803.

References

[1] S. Jin, T.H. Tiefel, M. McCormack, R.A. Fastnacht, R. Ramesh, L.H. Chen, Science 264 (1994) 413.
[2] P. Schiffer, A.P. Ramirez, W. Bao, S.W. Cheong, Phys. Rev. Lett. 75 (1995) 3336.
[3] M. Pekala, V. Drozd, J.F. Fagnard, Ph. Vanderbemden, J. Alloys Compd. 507 (2010) 350.
[4] A. Maignan, C. Martin, F. Damay, B. Raveau, Chem. Mater. 10 (1998) 950.
[5] W.S. Tan, H.P. Wu, K.M. Deng, X.S. Wu, Q.J. Jia, J. Gao, J. Alloys Compd. 491 (2010) 545.
[6] D.H. Manh, P.T. Phong, T.D. Thanh, L.V. Hong, N.X. Phuc, J. Alloys Compd. 491 (2010) 8.
[7] J. Pei, G. Chen, D.Q. Lu, P.S. Liu, N. Zhou, Solid State Commun. 146 (2008) 283.
[8] P. Xiang, Y. Kinemuchi, H. Kaga, K. Watari, J. Alloys Compd. 454 (2008) 364.
[9] D. Sousa, M.R. Nunes, C. Silveira, I. Matos, A.B. Lopes, M.E.M. Jorge, Mater. Chem. Phys. 109 (2008) 311.
[10] X.J. Fan, H. Koinuma, T. Hasegawa, Physica B 329–333 (2003) 723.
[11] C.S. Sanmathi, Y. Takahashi, D. Sawaki, Y. Klein, R. Retoux, I. Terasaki, J.G. Noudem, Mater. Res. Bull. 45 (2010) 558.
[12] Y. Zhou, I. Matsubara, R. Funahashi, G. Xu, M. Shikano, Mater. Res. Bull. 38 (2003) 341.
[13] N. Kumar, H. Kishan, A. Rao, V.P.S. Awana, J. Alloys Compd. 502 (2010) 283.
[14] Y. Wang, Y. Sui, P. Ren, L. Wang, X. Wang, W. Su, H. Fan, Inorg. Chem. 49 (2010) 3216.
[15] J.W. Park, D.H. Kwak, S.H. Yoon, S.C. Choi, J. Alloys Compd. 487 (2009) 550.
[16] R. Ang, Y.P. Sun, Y.Q. Ma, B.C. Zhao., X.B. Zhu, W.H. Song, J. Appl. Phys. 100 (2006) 063902.
[17] D. Flahaut, T. Mihara, R. Funahashi, N. Nabeshima, K. Lee, H. Ohta, K. Koumoto, J. Appl. Phys. 100 (2006) 084911.
[18] M. Ohtaki, H. Koga, T. Tokunaga, K. Eguchi, H. Arai, J. Solid State Chem. 120 (1995) 105.
[19] R. Funahashi, A. Kosuga, N. Miyasou, E. Takeuchi, S. Urata, K. Lee, H. Ohta, K. Koumoto, 26th International Conference on Thermoelectrics, IEEE, Piscataway, USA, 2007, p. 124.
[20] G. Zampieri, F. Prado, A. Caneiro, J. Briático, M.T. Causa, M. Tovar, B. Alascio, Phys. Rev. B 58 (1998) 3755.
[21] J. Briático, B. Alascio, R. Allub, A. Butera, A. Caneiro, M.T. Causa, M. Tovar, Phys. Rev. B 53 (1996) 14020.
[22] Z.Q. Yang, Q. Sun, L. Ye, X.D. Xie, Acta Phys. Sin. -EN ED 7 (1998) 851.
[23] F.P. Zhang, Q.M. Lu, X. Zhang, J.X. Zhang, J. Alloys Compd. 509 (2011) 542.
[24] I. Gil de Muro, M. Insausti, L. Lezama, T. Rojo, J. Solid State Chem. 178 (2005) 928.
[25] M.C. Payne, M.P. Teter, D.C. Allan, T.A. Arias, J.D. Joannopou los, Rev. Mod. Phys. 64 (1992) 1045.
[26] S.J. Clark, M.D. Segall, C.J. Pickard, P.J. Hasnip, M.J. Probert, K. Refson, M.C. Payne, Zeitschrift fuer Krystallographie 220 (5–6) (2005) 567.
[27] K. Takahata, Y. Iguchi, D. Tanaka, T. Itoh, I. Terasaki, Phys. Rev. B 61 (2000) 12551.
[28] S. Baroni, S. de Gironcoli, A. dal Corso, P. Giannozzi, Rev. Mod. Phys. 73 (2001) 515.

[29] J.C. Li, C.L. Wang, M.X. Wang, H. Peng, R.Z. Zhang, M.L. Zhao, J. Liu, J.L. Zhang, L.M. Mei, J. Appl. Phys. 105 (2009) 043503.
[30] M. Matsukawa, A. Tamura, Y. Yamato, T. Kumagai, S. Nimori, R. Suryanarayanan, J. Magn. Magn. Mater. 310 (2007) e283.
[31] G. Xu, R. Funahashi, M. Shikano, Q.Pu. Liu B., Solid State Commun. 124 (2002) 73.
[32] D.M. Rowe, C.M. Bhandari, Modern Thermoelectrics, Holt Saunders, London, 1983.
[33] T. Tsubota, T. Ohno, N. Shiraishi, Y. Miyazaki, J. Alloys Compd. 463 (2008) 288.
[34] M. Miclau, R. Hébert, C. Retoux, J. Martin, Solid State Chem. 178 (2005) 1104.
[35] L. Zhang, D.J. Singh, Phys. Rev. B 80 (2009) 075117.